

## EAS 6939 – Robust and Adaptive controls for Aerospace systems

### Medium Range Air to Air Missile (MRAAM) to a drone aircraft interception

Arif Mohammed

#### Introduction

In this project, an output feedback flight control system is designed and is integrated with a guidance law to intercept a Drone aircraft coming head on with a medium range air to air missile (MRAAM). Further the MRAAM is called a pursuer and the drone aircraft as a target.

The dynamic system of the pursuer is represented as

$$\dot{x} = Ax + Bu$$

$$y = Cx + Du$$

The pursuer is fired at an altitude of 40,000 ft at Mach 2.5. and the target is 20,000ft down range. The linearized equations of motion of a pursuer are

$$A = \begin{bmatrix} -1.57 & 0.00 & 0.00 & 1.00 & 0.00 \\ 0.00 & -0.50 & 0.17 & 0.00 & -1.00 \\ -21.13 & -2876.70 & -2.10 & -0.14 & -0.05 \\ -82.92 & -11.22 & -0.01 & -0.57 & 0.00 \\ -0.19 & -11.86 & -0.01 & 0.00 & -0.57 \end{bmatrix}$$

$$B = \begin{bmatrix} 0.00 & -0.10 & 0.00 \\ -0.07 & 0.00 & 0.11 \\ -1234.7 & -30.49 & -1803.2 \\ -4.82 & -119.65 & -7.00 \\ 14.84 & 0.27 & -150.58 \end{bmatrix}$$

State Vector:

$$x = [\alpha, \beta, p, q, r]$$

Control Input Vector

$$u = [\delta_a, \delta_e, \delta_r]$$

Control actuation system for the virtual control input,  $[\delta_a \delta_e \delta_r]$  are modelled as a second order system with the natural frequency  $\omega_n = 35$  Hz and a Damping ratio of  $\zeta = 0.71$ . The fins have a displacement of  $35^\circ$  and displacement limit of 350 deg/s.

From the above data the velocity of the pursuer will

$$V_0 = 2.5 * 967.5 \text{ ft/sec} = 2418.75 \text{ ft/sec}$$

Further as we treat the output of the aircraft longitudinal dynamics  $A_z$  and the other accessible outputs will be the roll rates then the output vector is constituted as follows:

$$y = [A_z \ p \ q \ r]$$

then the output matrices for State space model can be computed as follows:

$$C = \begin{bmatrix} Z_\alpha & 0 & 0 & 0 & 0 \\ 0 & 0 & 1 & 0 & 0 \\ 0 & 0 & 0 & 1 & 0 \\ 0 & 0 & 0 & 0 & 1 \end{bmatrix}, \quad D = \begin{bmatrix} 0 & Z_\delta & 0 \\ 0 & 0 & 0 \\ 0 & 0 & 0 \\ 0 & 0 & 0 \end{bmatrix}$$

We can compute the values of  $Z_\alpha$  and  $Z_\delta$  from the given equation of motion:

$$Z_\alpha = -1.57 * V_0 = -1.57 * 2418.75 = -3797.44$$

$$Z_\delta = -0.10 * V_0 = -0.10 * 2418.75 = -241.87$$

The open eigen values of the system are computed and are as follows:

$$-1.2895 + 21.8316i,$$

$$-1.2895 - 21.8316i,$$

$$-1.0695 + 9.0870i,$$

$$-1.0695 - 9.0870i,$$

$$-0.5920 + 0.0000i$$

It is evident from the eigen values that the open loop system is stable as all the poles lie in the strict left half plane. The eigen values closest to the imaginary axis i.e.,  $-0.5920$  corresponds to the highly damped slow roll subsidence mode, the eigen values farthest to from the imaginary axis i.e.,  $-1.2895 \pm 21.8316i$  corresponds to the lightly damped fast Dutch roll mode. While the eigen values in between i.e.,  $-1.0695 \pm 9.0870i$  corresponds to the short period dynamics.

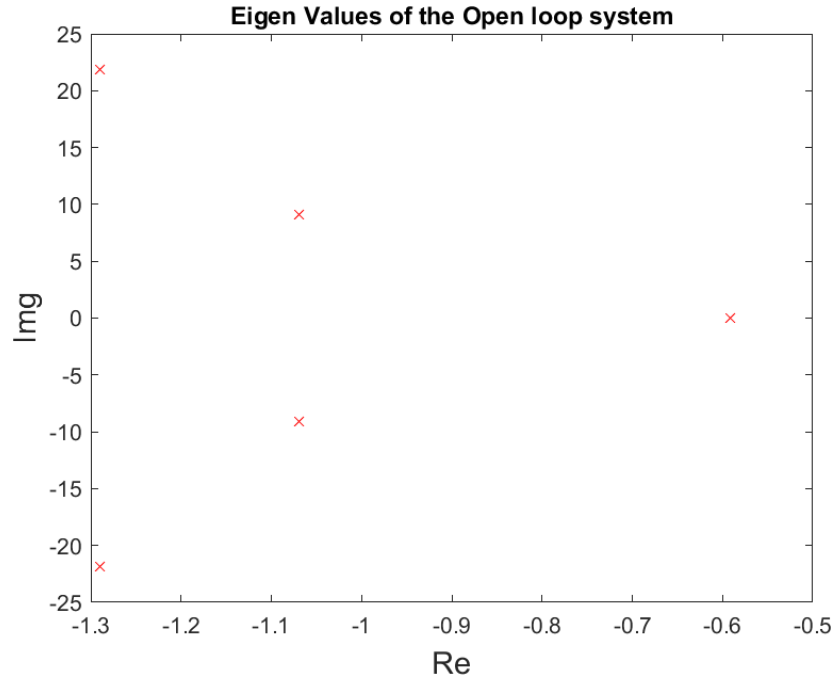


Figure 1 Eigen Values of the Pursuer open loop system

### Short Period Dynamics

The short period dynamics are extracted from the given system dynamics and are as follows:

$$\begin{bmatrix} \dot{\alpha} \\ \dot{q} \end{bmatrix} = \begin{bmatrix} -1.57 & 1 \\ -82.92 & -0.57 \end{bmatrix} \begin{bmatrix} \alpha \\ q \end{bmatrix} + \begin{bmatrix} -0.1 \\ -119.65 \end{bmatrix} \delta_e$$

Computing the Vertical acceleration of the short period dynamics

$$A_z = Z_\alpha \alpha + Z_\delta \delta_e$$

$$\begin{bmatrix} A_z \\ q \end{bmatrix} = \begin{bmatrix} -3797.4 & 0 \\ 0 & 1 \end{bmatrix} \begin{bmatrix} \alpha \\ q \end{bmatrix} + \begin{bmatrix} -241.8750 \\ 0 \end{bmatrix} \delta_e$$

The eigen values of the short period dynamics are  $-1.07 \pm 9.0923i$  which approximately equal to the eigen values computed from the complete dynamic system of the pursuer.

## Approach

### Control Design model:

Asymptotic tracking is achieved by embedding the command model  $\dot{r} = 0$  into the short period dynamics. As a result, the following robust servomechanism design model is obtained,

$$\begin{bmatrix} \ddot{e}_{I,A_z} \\ \ddot{\alpha} \\ \ddot{q} \end{bmatrix} = \begin{bmatrix} 0 & -3797.44 & 0 \\ 0 & -1.57 & 1 \\ 0 & -82.92 & -0.57 \end{bmatrix} \begin{bmatrix} \dot{e}_{I,A_z} \\ \dot{\alpha} \\ \dot{q} \end{bmatrix} + \begin{bmatrix} -241.875 \\ -0.1 \\ -119.65 \end{bmatrix} \dot{\delta}_e(t)$$

Also denoted  $\dot{z} = \tilde{A}z + \tilde{B}\mu$  where  $\mu = \dot{\delta}_e$ ,  $z = [\dot{e}_{I,A_z}, \xi(t)^T]^T$ ,  $\xi = [\dot{\alpha}, \dot{q}]^T$ ,

$$e_{A_z} = A_z - A_{z,cmd} \text{ and } e_{I,A_z} = \int_{t_0}^t e_{A_z}(\tau) \tau.$$

Applying the infinite horizon linear quadratic regulator (LQR) to the servo mechanism design model determines for the state feedback law,  $\mu(t) = \dot{u} = -K * z(t)$ , where  $K = [K_{\ddot{e}_{I,A_z}}, K_{\ddot{\alpha}}, K_{\ddot{q}}]$ . Assuming the state feedback gains are constant, integrating once gives

$$\begin{aligned} \delta_e(t) &= -K_{\ddot{e}_{I,A_z}} \int_{t_0}^t e_{A_z}(\tau) \tau - K_{\ddot{\alpha}} \alpha - K_{\ddot{q}} q + c \\ &= - \begin{bmatrix} -K_{\ddot{e}_{I,A_z}} & K_{\ddot{\alpha}} & K_{\ddot{q}} \end{bmatrix} \begin{bmatrix} e_{I,A_z} \\ \alpha \\ q \end{bmatrix} \end{aligned}$$

Where the gains subscripts have been, maintained for clarity but could be renamed according to the integrated terms they multiply. Also, c is constant of integration that can be neglected because the embedded command model  $\dot{r} = 0$ , provides robustness to additive disturbances to the plant,  $\dot{\omega} = 0$ . The architecture is illustrated in Figure 2.

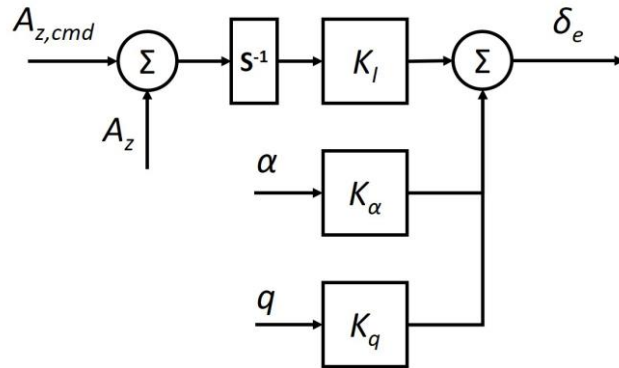


Figure 2: Proportional integral control architecture resulting from the robust servo mechanism design model

### Control Tuning:

Elements of the infinite time LQR penalty matrices  $Q$  or  $R$  can be systematically adjusted to increase control effort. However, more control effort does not necessarily imply a faster response since open loop zeros can create dominant closed loop poles. To investigate, the control penalty matrix was chosen as  $R = 1$  and the state penalty matrix was set to,

$$Q = \begin{bmatrix} q_{el} & 0 & 0 \\ 0 & 0 & 0 \\ 0 & 0 & 0 \end{bmatrix}$$

where the integral error penalty,  $q_{el}$  was incrementally increased from  $10^{-8}$  to  $10^{-4}$ , spaced linearly on a logarithmic scale over 30 points. These matrices also ensure that  $Q \geq 0$ ,  $R > 1$ , and  $(\tilde{A}, Q)$  is observable and  $(\tilde{A}, \tilde{B})$  is controllable.

### Actuator Dynamic:

The analysis model includes an 2nd order actuator with natural frequency  $\omega_n = 35\text{Hz}$  and damping ratio  $\zeta = 0.71$ . The Fin displacement and the Fin displacement rates depend on the actuator dynamics.

$$\begin{bmatrix} \dot{\delta}_e \\ \ddot{\delta}_e \end{bmatrix} = \begin{bmatrix} 0 & 1 \\ -\omega_n^2 & -2\zeta\omega_n \end{bmatrix} \begin{bmatrix} \delta_e \\ \dot{\delta}_e \end{bmatrix} + \begin{bmatrix} 0 \\ \omega_n^2 \end{bmatrix} \delta_{cmd}$$

As the full state feedback is not available using the analysis model, state estimates  $\hat{e}_{I,A_z}$ ,  $\hat{\alpha}$ ,  $\hat{q}$  obtained using an observer, yielding controller

$$\begin{aligned} \delta_e &= -\begin{bmatrix} K_{eI,A_z} & K_\alpha & K_q \end{bmatrix} \begin{bmatrix} \hat{e}_{I,A_z} \\ \hat{\alpha} \\ \hat{q} \end{bmatrix} \\ &= -K_c \hat{X} \end{aligned}$$

The objective is to design the LQR gain  $K_c$  using the state space model with  $e_{I,A_z}$  as an additional state. The state space model  $(A_I, B_{I1}, B_{I2}, C_I, D_{I1}, D_{I2})$  yielding output  $e_{I,A_z}$  with  $A_z, q$  as input is given by

$$\begin{aligned} \dot{e}_{I,A_z} &= [0] + [1 \ 0] \begin{bmatrix} A_z \\ q \end{bmatrix} + [-1] A_{z,cmd} \\ \begin{bmatrix} e_{I,A_z} \\ q \end{bmatrix} &= \begin{bmatrix} 1 \\ 0 \end{bmatrix} e_{I,A_z} + \begin{bmatrix} 0 & 0 \\ 0 & 1 \end{bmatrix} \begin{bmatrix} A_z \\ q \end{bmatrix} + \begin{bmatrix} 0 \\ 0 \end{bmatrix} A_{z,cmd} \end{aligned}$$

To build an observer with the state estimates  $\hat{x}$ , we need to consider a model which has  $x = [x_I \ x_p]^T$  as a state. Such a model is constructed by combining plant, observer, actuator to form dynamic compensator  $(A, B_1, B_2, C, D_1, D_2)$

$$\begin{bmatrix} \dot{x}_I \\ \dot{x}_p \end{bmatrix} = \begin{bmatrix} A_I & B_{I1}C_p \\ 0 & A_p \end{bmatrix} \begin{bmatrix} x_I \\ x_p \end{bmatrix} + \begin{bmatrix} B_{I1}D_p \\ B_p \end{bmatrix} \delta_e + \begin{bmatrix} B_{I2} \\ 0 \end{bmatrix} A_{z,cmd}$$

$$y_I = [C_I \ D_{I1}C_p] \begin{bmatrix} x_I \\ x_p \end{bmatrix} + D_{I1}D_p\delta_e + D_{I2}A_{z,cmd}$$

Where  $x_I = e_{I,A_z}$   $x_p = [\alpha \ q]^T$ ,  $y_I = [e_{I,A_z} \ q]^T$ . The terms  $D_1, D_2$  have all entries zero, in the observer design analysis. Based on these dynamics, Luenberger observer is designed as

$$\begin{aligned} \dot{\hat{x}} &= A\hat{x} + B_1u + B_2r + L(y - C\hat{x}) \\ &= A\hat{x} - B_1K_c\hat{x} + L(y - C\hat{x}) \\ &= (A - B_1K_c - LC)\hat{x} + B_2r + Ly \end{aligned}$$

Defining the observer error  $\tilde{x} = x - \hat{x}$ , the observer dynamics are

$$\begin{aligned} \dot{\tilde{x}} &= \dot{x} - \dot{\hat{x}} \\ &= Ax + B_1u + B_2r - A\hat{x} - Bu - B_2r - L(y - C\hat{x}) \\ &= (A - LC)\tilde{x} \end{aligned}$$

The observer gains L is tuned using LQR method with  $A^T, C^T$  replacing and penalties  $Q_0 = q_0I_3, R_0 = I_2$ , where the parameter  $q_0$  can be tuned. The combined controller and observer dynamics can be written as

$$\begin{bmatrix} \dot{x}_I \\ \dot{\hat{x}} \end{bmatrix} = \begin{bmatrix} A_I & 0 \\ LC_I & A_0^{cl} \end{bmatrix} \begin{bmatrix} x_I \\ \hat{x} \end{bmatrix} + \begin{bmatrix} B_{I1} \\ LD_I \end{bmatrix} y_p + \begin{bmatrix} B_{I2} \\ B_2 \end{bmatrix} A_{z,cmd}$$

$$\delta_{cmd} = [0 \ -K_c] \begin{bmatrix} x_I \\ \hat{x} \end{bmatrix} + [0 \ 0 \ 0]^T y_p + [0] r.$$

### Design Charts:

The design charts are created for the state feedback controller and the dynamic compensator according to time and frequency domain requirements. The controller LQR penalty matrix

$$Q = \begin{bmatrix} q_{el} & 0 & 0 \\ 0 & 0 & 0 \\ 0 & 0 & 0 \end{bmatrix}; \ R = 1$$

With the values of  $q_{el}$  ranging from  $10^{-8}$  to  $10^{-4}$  on *logscale*, with 30 data points, and the design charts are created with respect to the corresponding crossover frequencies and  $q_{11}$ . The observer penalty  $q_0$  is iterated on a scale of 1 to  $10^4$  with 30 points and after iterations

$$w = 1000 * \begin{bmatrix} 1 & 0 & 0 \\ 0 & 1 & 0 \\ 0 & 0 & 1 \end{bmatrix}$$

$$v = \begin{bmatrix} 1 & 0 \\ 0 & 1 \end{bmatrix}$$

and verifications of the design characteristics the penalty is fixed at 1000. For creating the design charts a step acceleration of 20g is considered for all the time domain requirements as worst-case scenario.

### Design charts for state feedback controller:

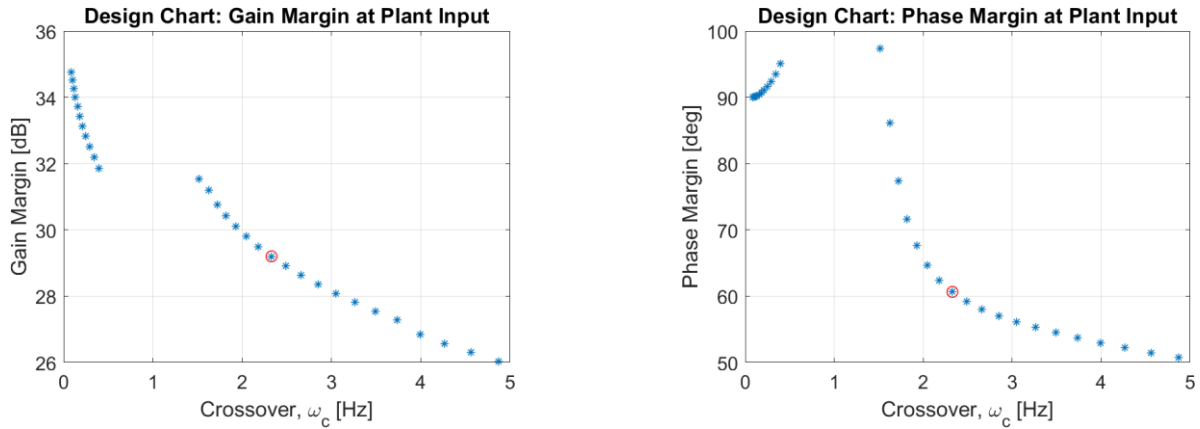


Figure 3 Gain margin and phase margin plots for state feedback controller.

The gain margin is above 6dB and the phase margin is above 35 degrees for the state feedback controller for the entire range of crossover frequencies.

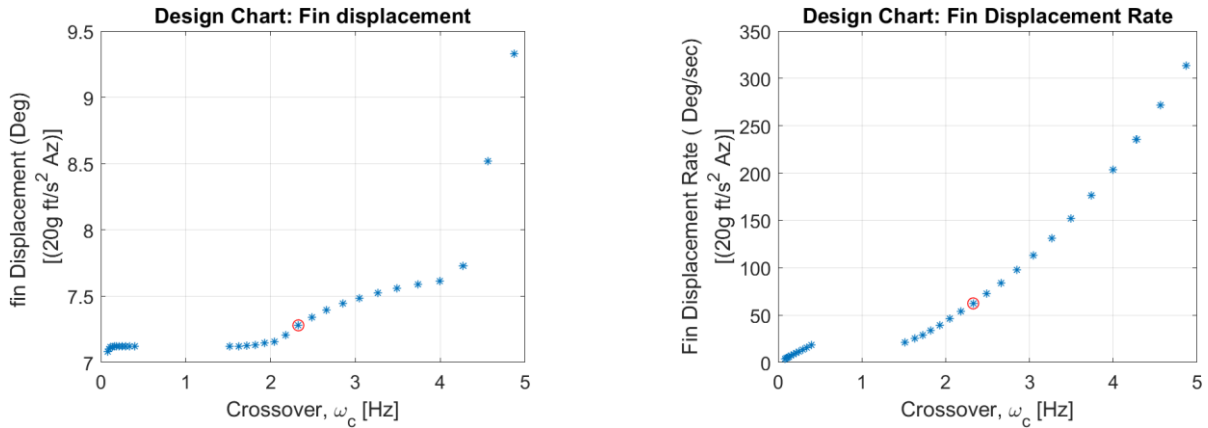


Figure 4 Fin displacement and fin displacement rate plots for state feedback controller

The fin displacement is below 35 degrees for the entire range of cross over frequencies and penalty  $q_{el}$ . The fin displacement is below 350 degrees per second for the entire range of cross over frequencies and penalty  $q_{el}$ .

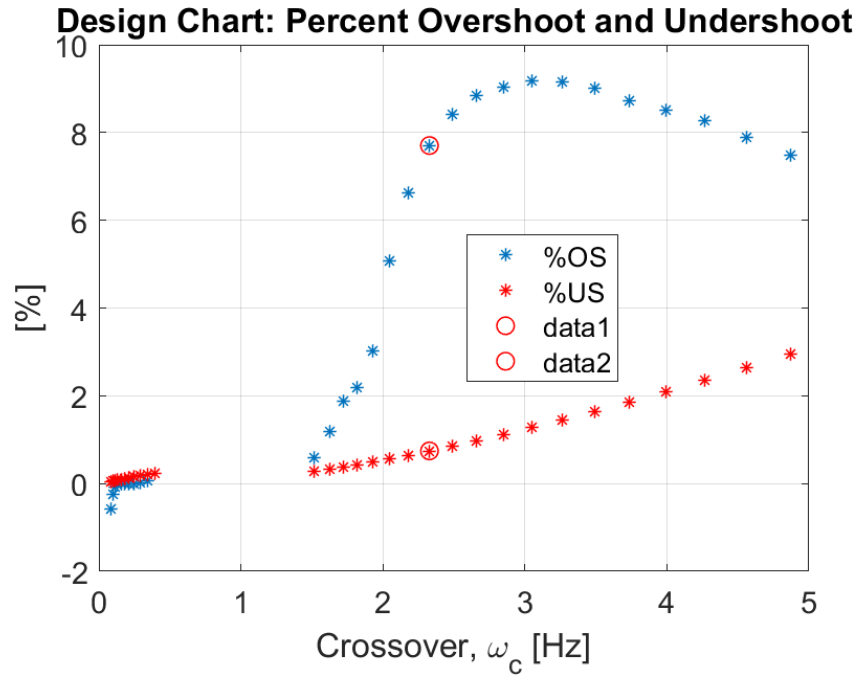


Figure 5 Overshoot and Undershoot plots for state feedback controller

The percentage of peak overshoot and undershoot is below 10% for the state feedback controller in the entire range of cross over frequencies

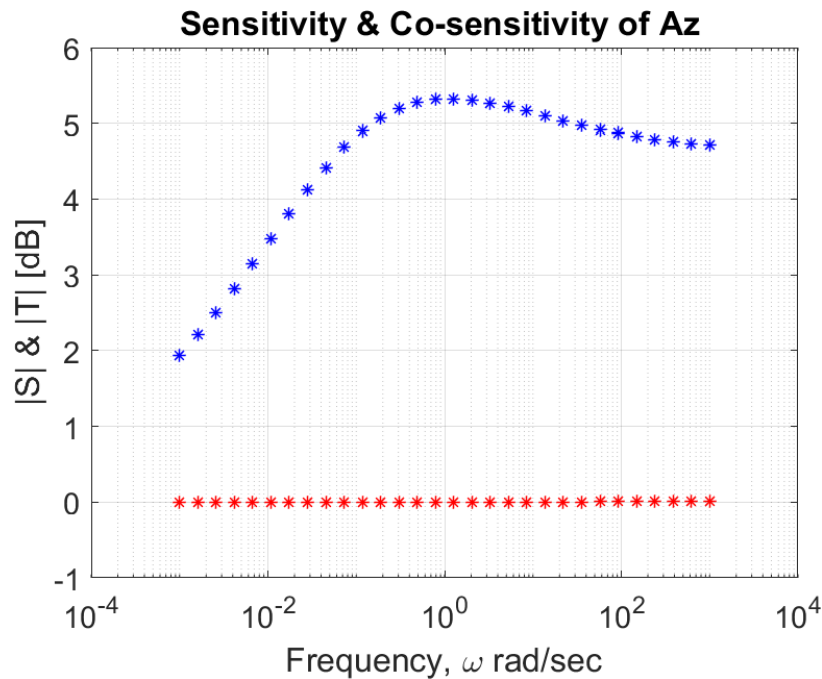


Figure 6 Sensitivity and complimentary sensitivity  $A_z$  plots for state feedback controller

The Sensitivity and complimentary sensitivity of the  $A_z$  is below 6dB for the frequency range of  $10^{-3}$  to  $10^3$  rad/sec.



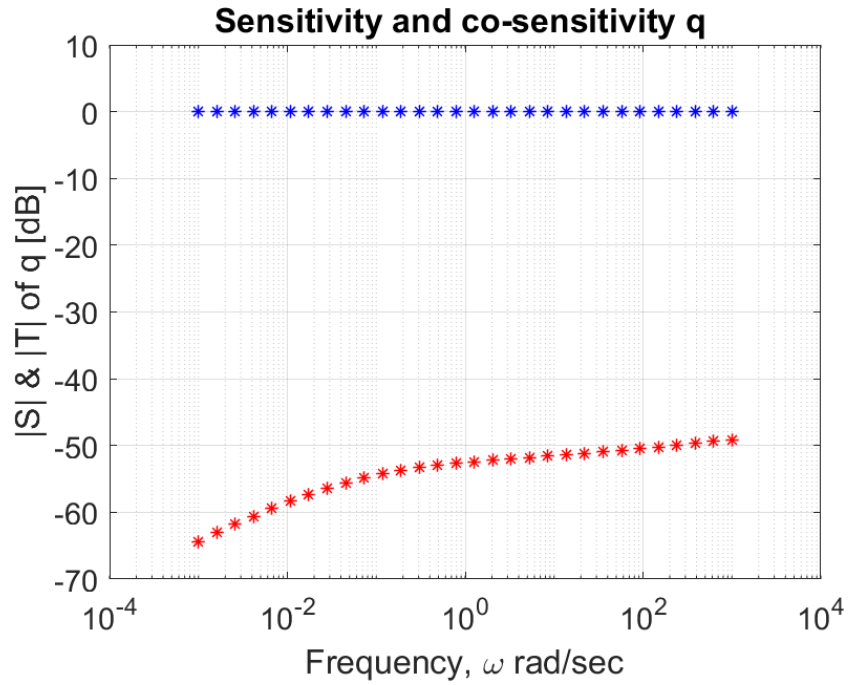


Figure 7 Sensitivity and complimentary sensitivity of  $q$  plots for state feedback controller

The Sensitivity and complimentary sensitivity of the  $q$  is below 6dB for the frequency range of  $10^{-3}$  to  $10^3$  rad/sec for the state feedback controller.

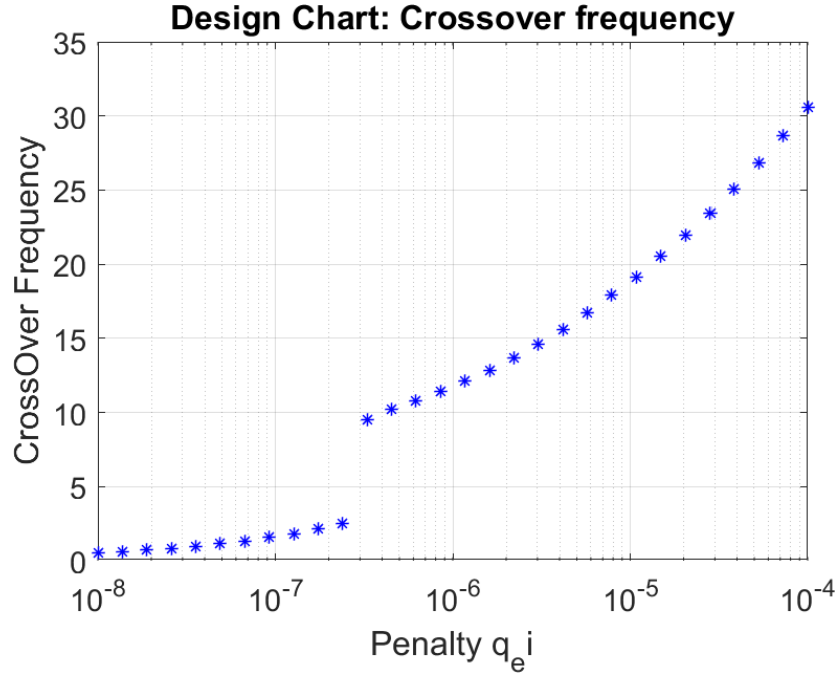


Figure 8 loop cross Over frequency plot for state feedback controller

Loop gain input crossover frequency is less than  $1/3^{\text{rd}}$  the actuator natural frequency which is 73.3038 rad/sec.

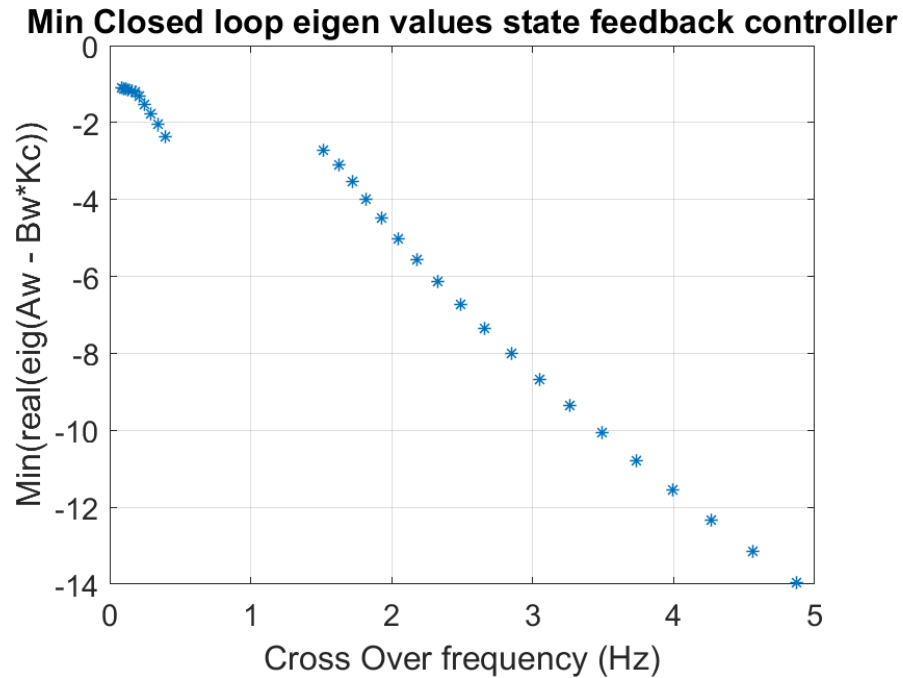


Figure 9 Minimum real part of closed loop eigen values state feedback controller

The real part of closed loop eigen values for state feedback controller is always greater than -500 for all the values of the cross over frequency.

**Design Charts for Observer model with actuator, controller in loop:**

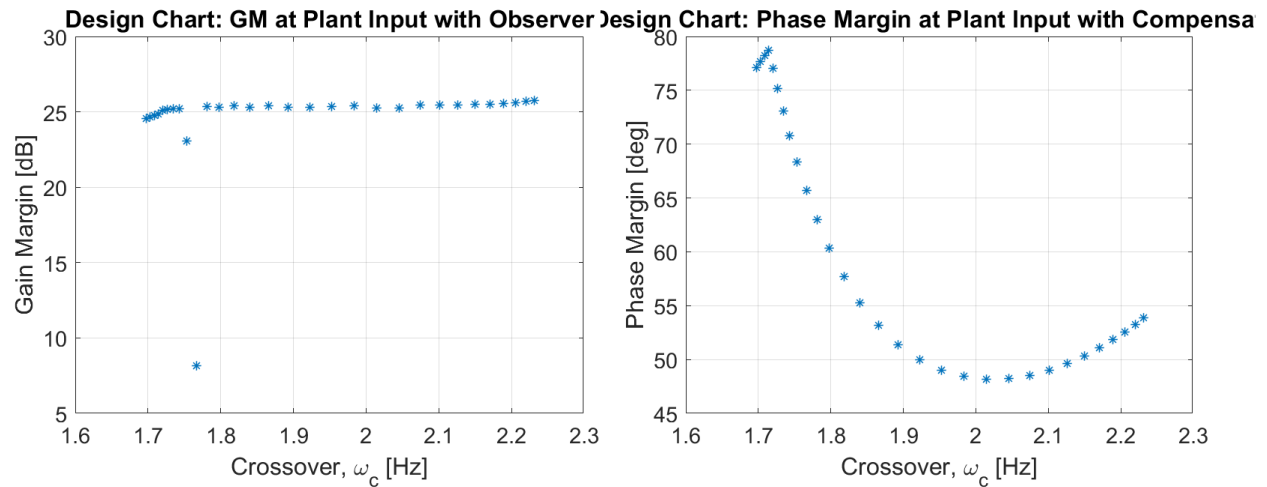


Figure 10 Gain and Phase margin for Observer model

The gain margin is always above 6db and the phase margin is above 35 dB for all the frequency ranges.

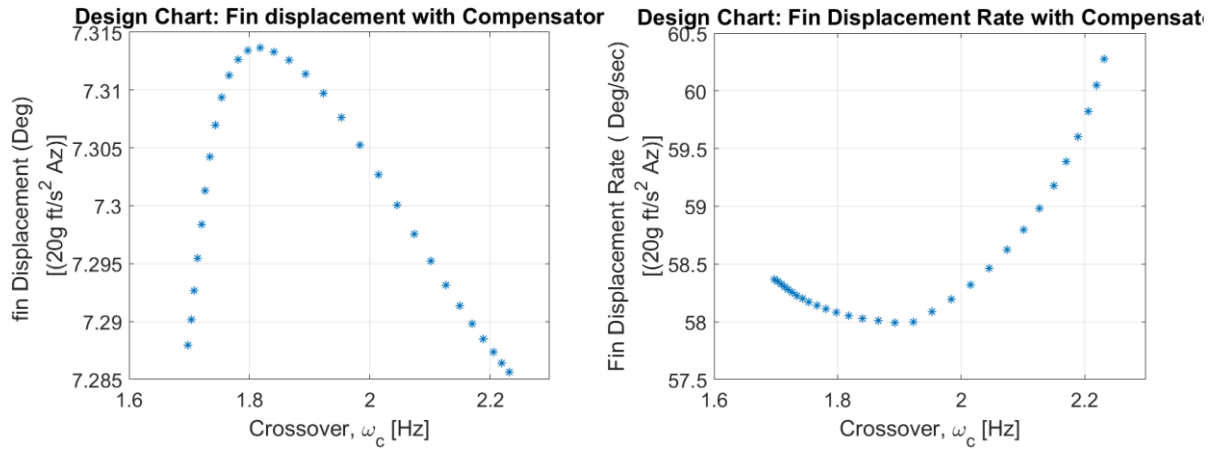


Figure 11 Fin displacement and fin displacement rate with observer in loop.

Maximum fin displacement is well under 35degrees, and maximum fin displacement rate is below 350 deg/sec with observer in loop. This acceptable as per desired frequency domain analysis.

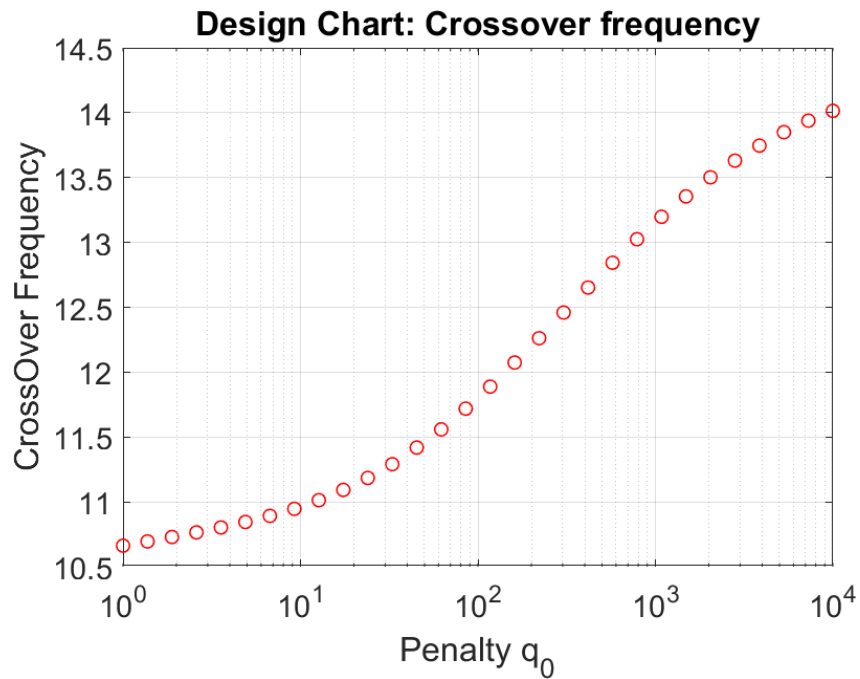


Figure 12 loop cross Over frequency plot for observer in loop

Loop gain input crossover frequency is less than 1/3<sup>rd</sup> the actuator natural frequency which is 73.3038 rad/sec for the entire range of the observer penalties  $q_o$ .

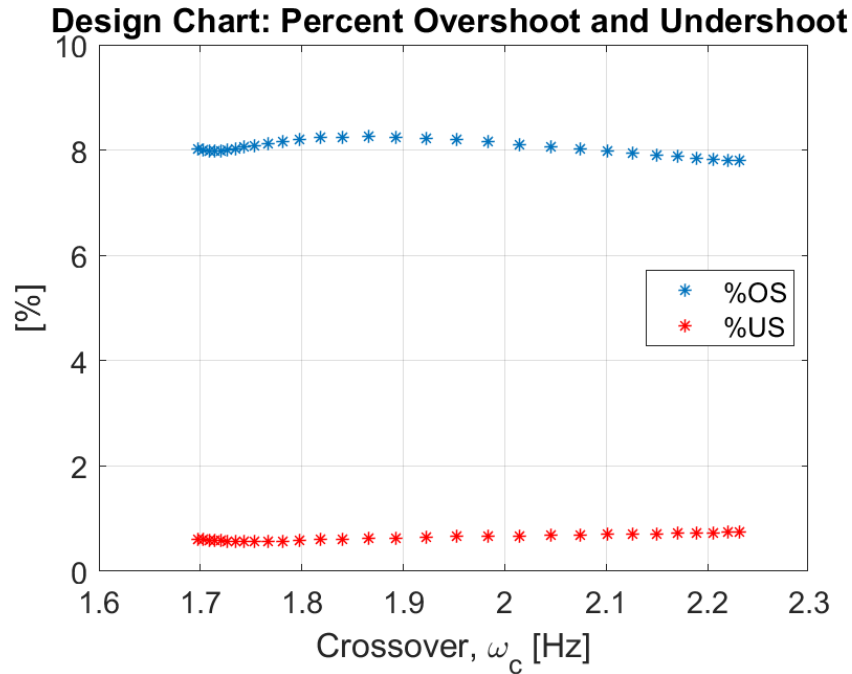


Figure 13 Overshoot and Undershoot plots with observer in loop

The percentage of overshoot and undershoot for the Analysis model with observer in loop is always below 10% which is desired phenomena.

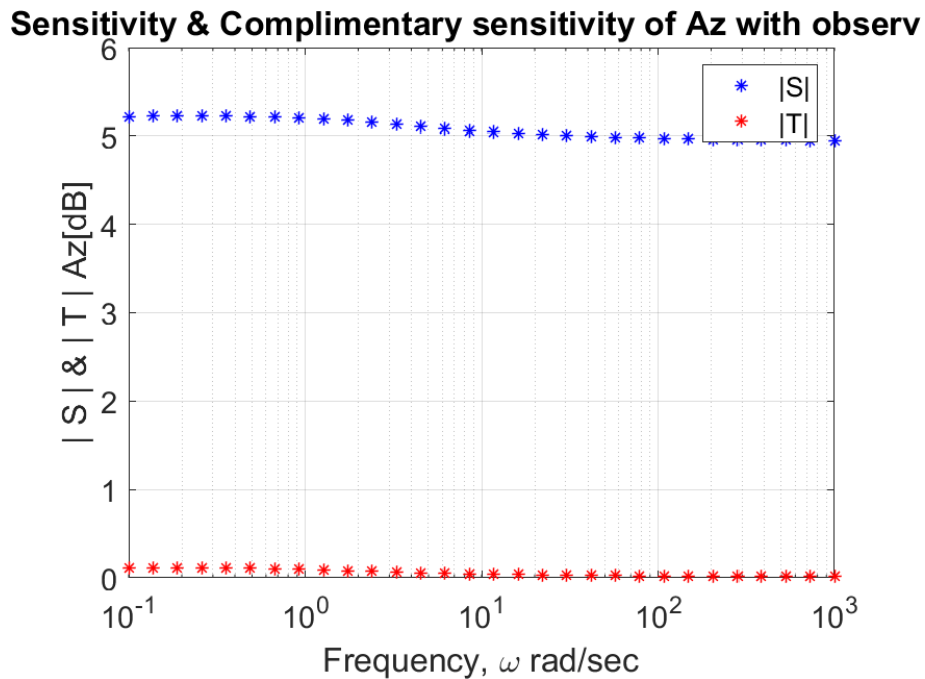


Figure 14 Sensitivity and Complimentary sensitivity plots for  $A_z$  with observer in loop

The sensitivity and complimentary sensitivity for  $A_z$  of the system with observer is well below 6dB as per requirements.

**Sensitivity & Complimentary sensitivity of q with observe**

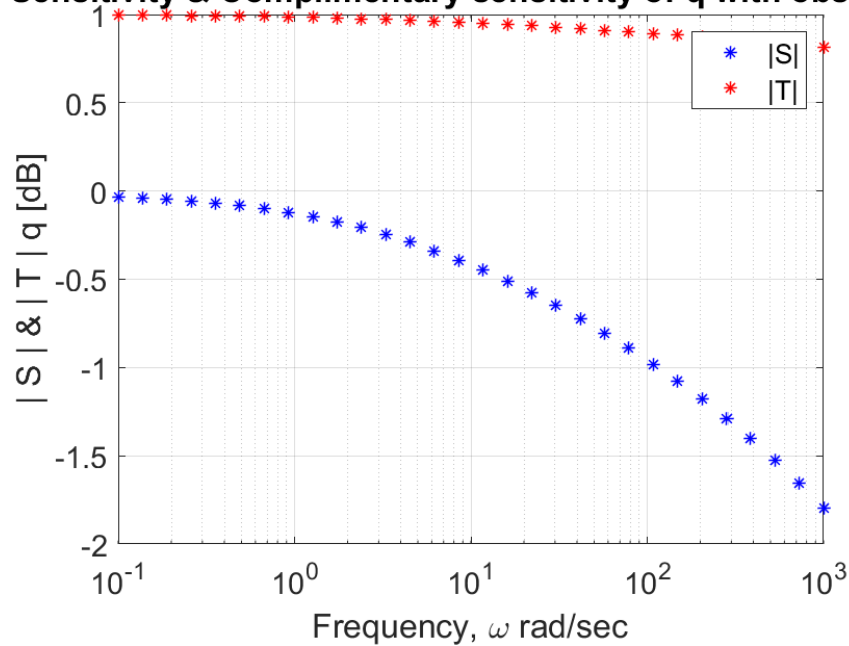


Figure 15 Sensitivity and Complimentary sensitivity plots for  $q$  with observer in loop

The sensitivity and complimentary sensitivity for  $q$  of the system with observer is well below 6dB as per requirements.

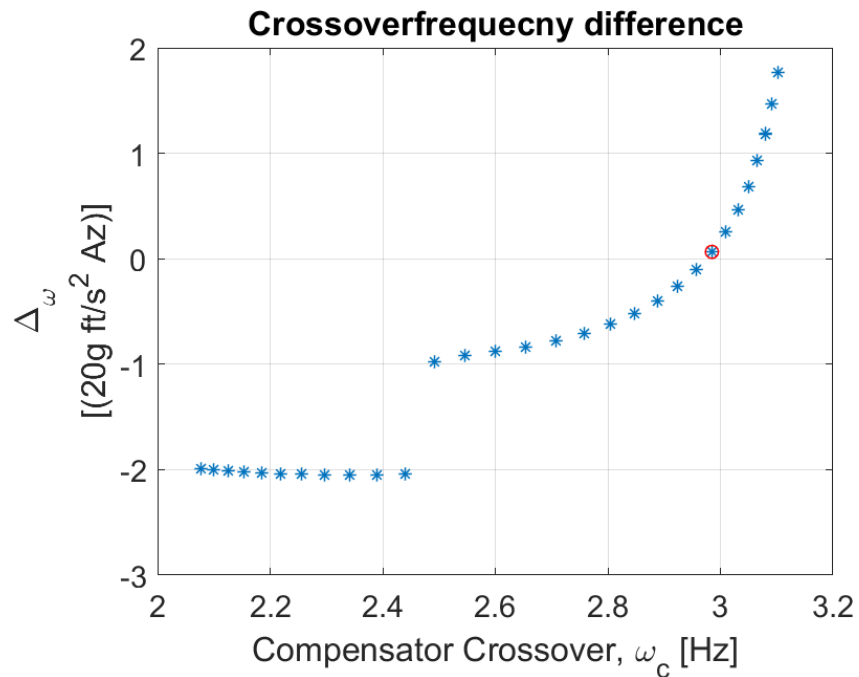


Figure 16 Difference between Compensator and LQR loop gain crossover frequencies

The difference between the cross over frequencies of compensator and LQR loop gains is below 0.25 Hz for the crossover frequency of under 2.9849 Hz or 18.7547 rad/sec.

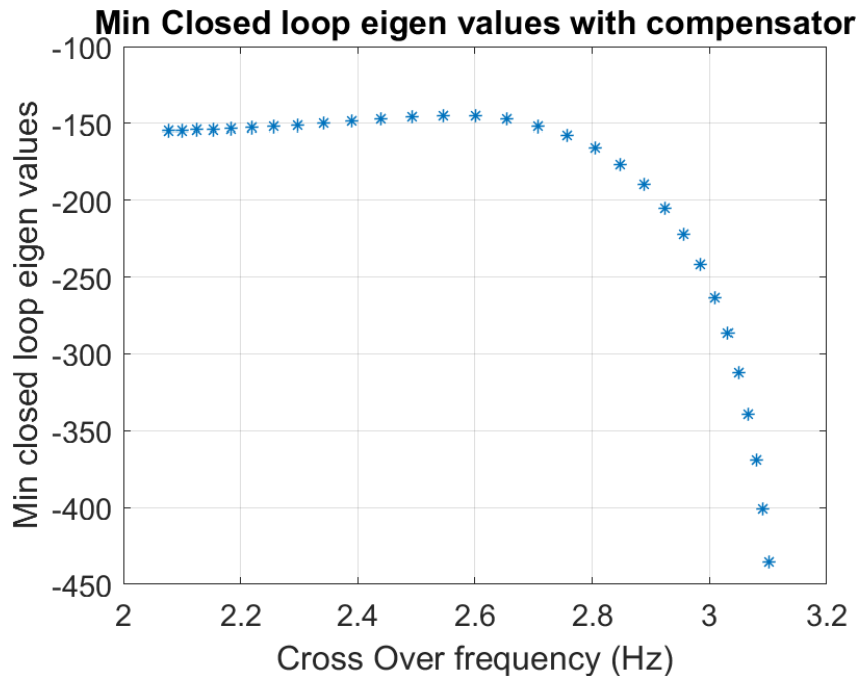


Figure 17 Minimum of real part of closed loop eigen values with the observer

It is evident from the graph that all the eigen values are higher than -500 for the entire range of the cross over frequencies satisfying the need requirements.

From the figure 3-15 the all the requirements are satisfied for the entire range of the cross over frequencies except the compensator loop gain and LQR loop gain difference which only satisfies for the frequencies below 2.9849 Hz or 18.7547 rad/sec which is the 23 points in the frequency range parts of 30.

From this we can select any point for LQR gains and below point 23 for the Compensator gains.

## Part 2: Drone Intercept simulation

The objective is to directly hit the drone therefore the missile is tuned such that the miss distance is as low as possible and preventing the actuator a saturation.

Given Data:

Initial conditions

Altitude  $R_{Tz}^i$  RT2 = 40000 ft.

Velocity  $V_T^i$  VT = 300 ft/sec.

Heading error, HE = -20 degrees

Drone acceleration nT =  $3g = 3 \times 32.1741 = 96.5223 \text{ ft/sec}^2$

Limitations  $VP \leq 20 g$

Missile velocity  $V_M^i$  VM = 2.5 Mach =  $2.418.8 \frac{ft}{sec^2}$

Horizontal position of target in inertial frame  $R_{Tx}^i$  RT1 = 20000 ft.

vertical position of target in inertial frame  $R_{Tz}^i$  RT2 = 40000.ft.

Target flight path  $\beta = 0^\circ$

For target,  $\dot{\beta} = \frac{a_T^t}{V_{Tx}^t}$

$$\dot{R}_{Tx}^i = V_{Tx}^i$$

$$\dot{R}_{Tz}^i = V_{Tz}^i$$

$$V_{Tx}^i = -V_{Tx}^t \cos(\beta)$$

$$V_{Tz}^i = V_{Tx}^t \sin(\beta)$$

$$\dot{V}_{Tx}^i = a_{Tz}^t \sin(\beta)$$

$$\dot{V}_{Tz}^i = a_{Tz}^t \cos(\beta)$$

For the missile dynamics

$$a_{Mx}^i = -a_{Mz}^m \sin(\lambda)$$

$$a_{Mz}^i = -a_{Mz}^m \cos(\lambda)$$

$$\dot{R}_{Mx}^i = V_{Mx}^i$$

$$\dot{R}_{Mz}^i = V_{Mz}^i$$

$$\dot{R}_{\frac{T}{M}}^i = R_M^i - R_T^i$$

the closing velocity  $V_c = \frac{-R_{TMx}^i V_{TMx}^i - R_{TMz}^i V_{TMz}^i}{\left| R_{\frac{T}{M}} \right|^2}$

the expression for  $\dot{\lambda} = \frac{R_{TMx}^i V_{TMz}^i - R_{TMz}^i V_{TMx}^i}{\left| R_{\frac{T}{M}} \right|^2}$

For true navigation  $a_M^{true} = NV_c \dot{\lambda}$

Where N is the navigation gain.

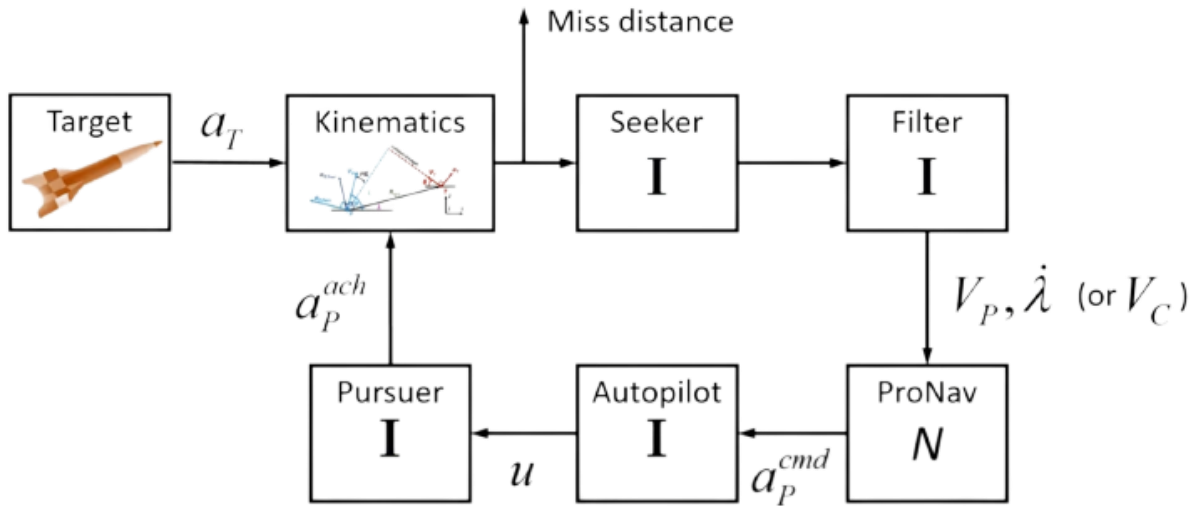


Figure 18 Homing Loop architecture with Autopilot

From the design charts the Dynamic compensator is developed and the State space matrices of the dynamic compensator are saved and loaded into guidance part to prevent rerunning simulation of whole Autopilot system. Then the Homing loop is simulated with the Pursuer gains ranging from 4 – 7 and it was found from the figures that the trajectory with the  $N_p = 7$  was optimal but the actuator input is saturated, and we go ahead with the dynamics. Initially the purely longitudinal scenario with nonlinear proportional navigation law was simulated with the control gains of [ 4, 5, 6] and the trajectories were chosen as follows:

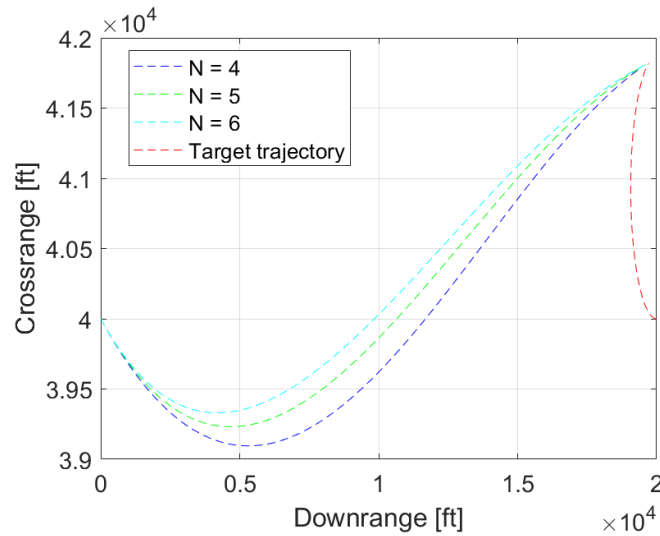


Figure 19 Initial trajectories without auto pilot.



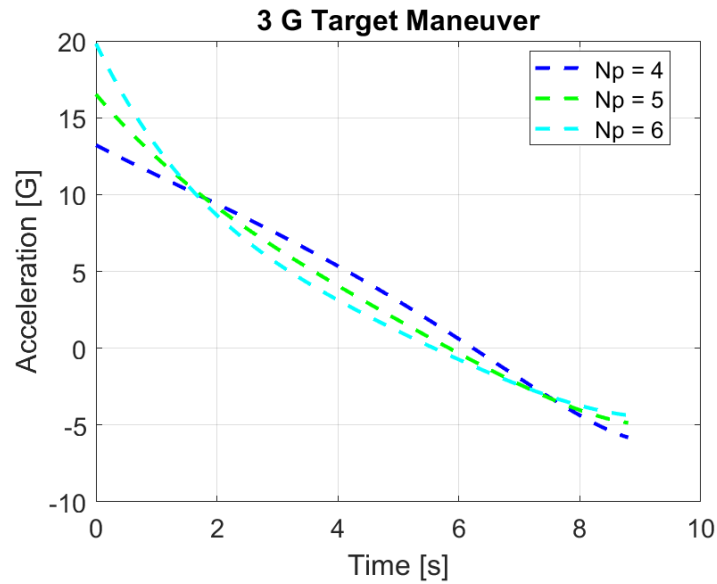


Figure 20 Target Maneuver plot without auto pilot.

The criteria for selecting the Pursuer gain are that missile should intercept the target as soon as possible and the Acceleration does not exceed 20g. so from figure it is evident that the best gain would be 6. For the gain 6 the target missed with 57.0246 ft as shown in figure 21

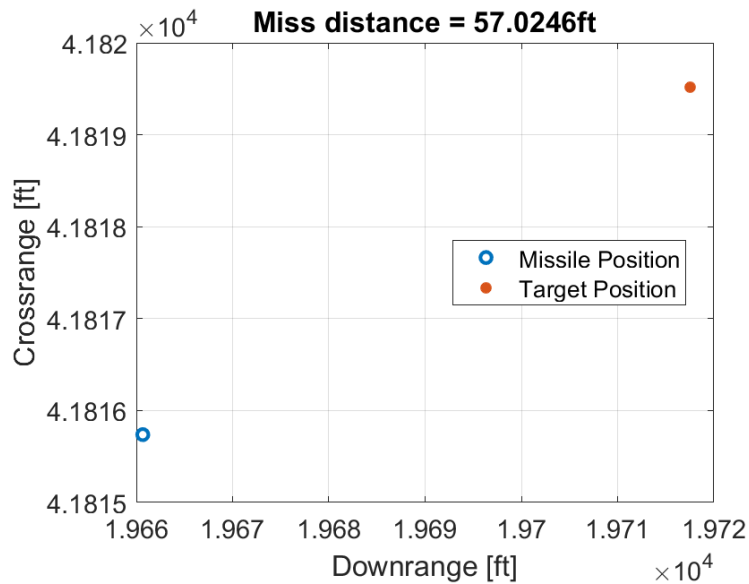


Figure 20 Miss Distance plot without auto pilot.

Further the Autopilot is integrated by selecting the gain as 5.9599 and the final time as 8.83009 sec. Then trial and was carried out for various penalties of the controller and The Compensator looking for least miss distance.

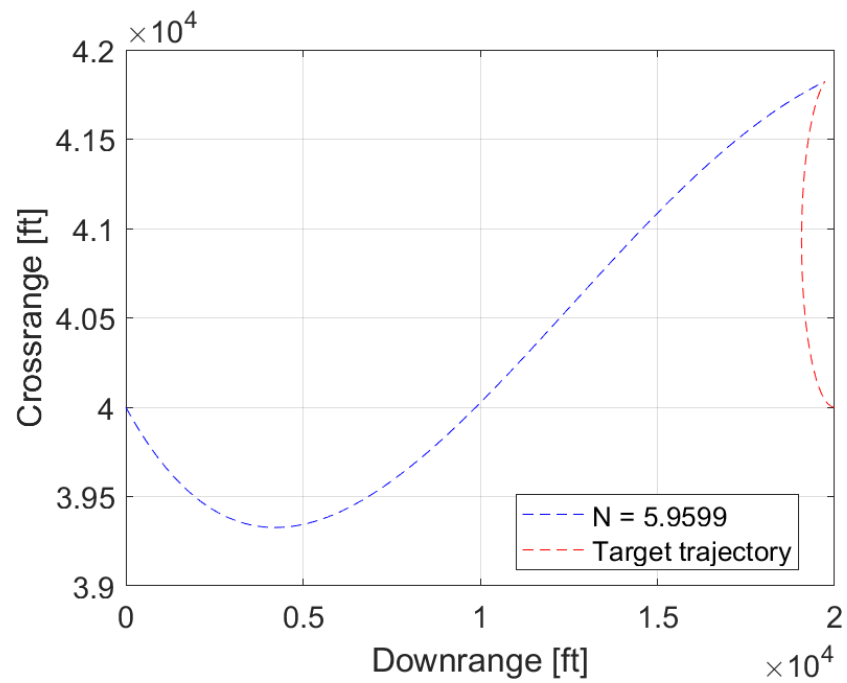


Figure 21 Optimized trajectory of Pursuer and Target.

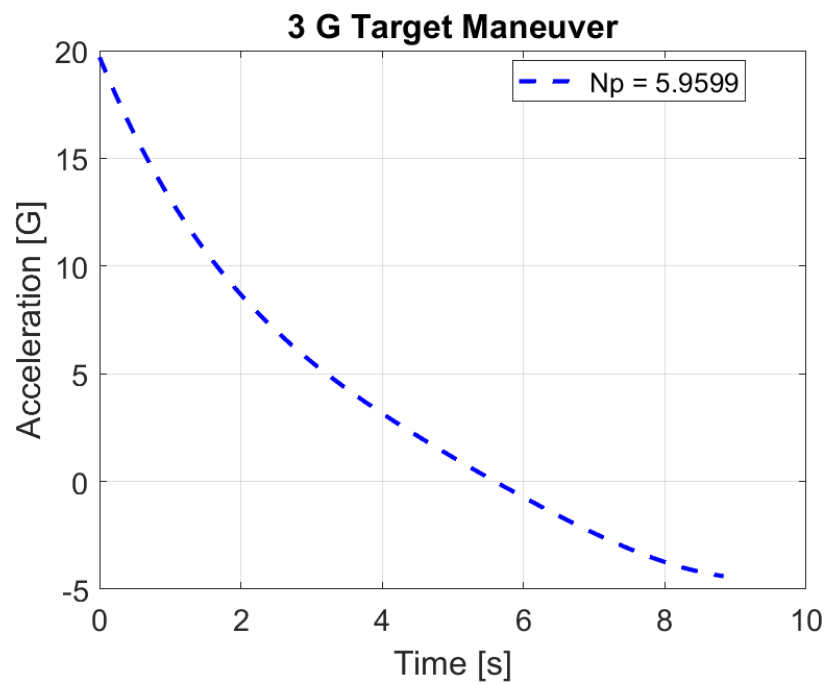


Figure 22 3g target maneuver for pursuer gain of 5.9599.

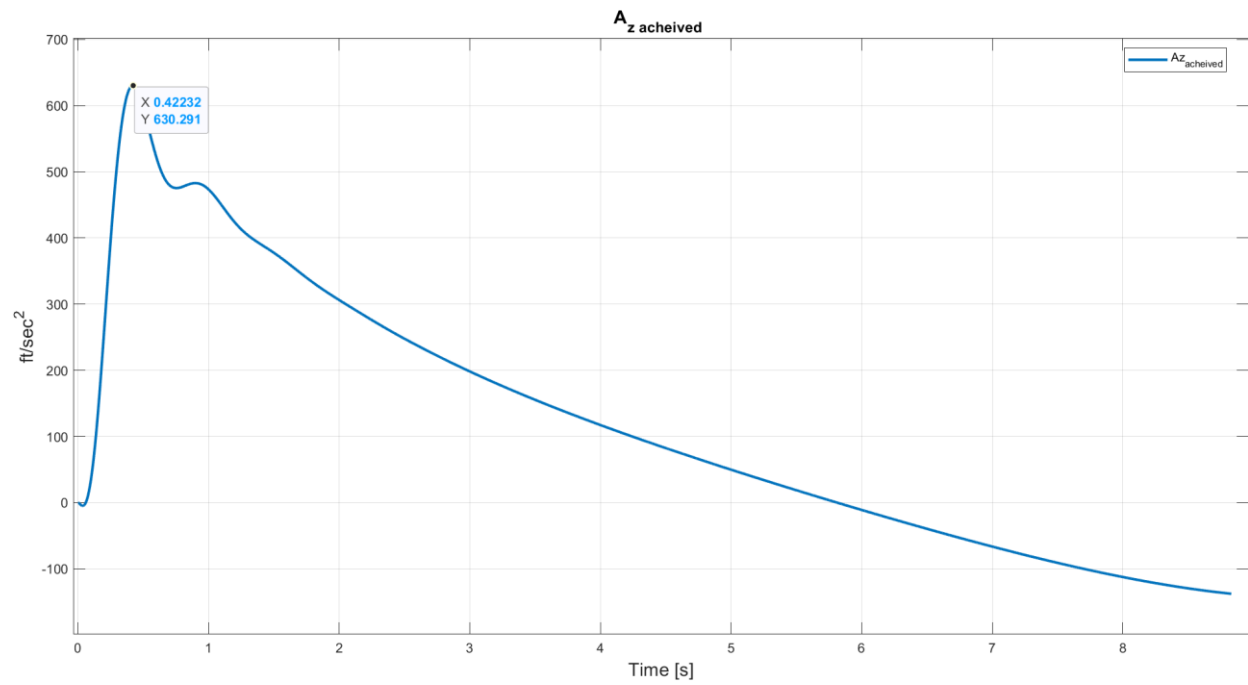


Figure 23 Acceleration achieved by pursuer within 20g range.

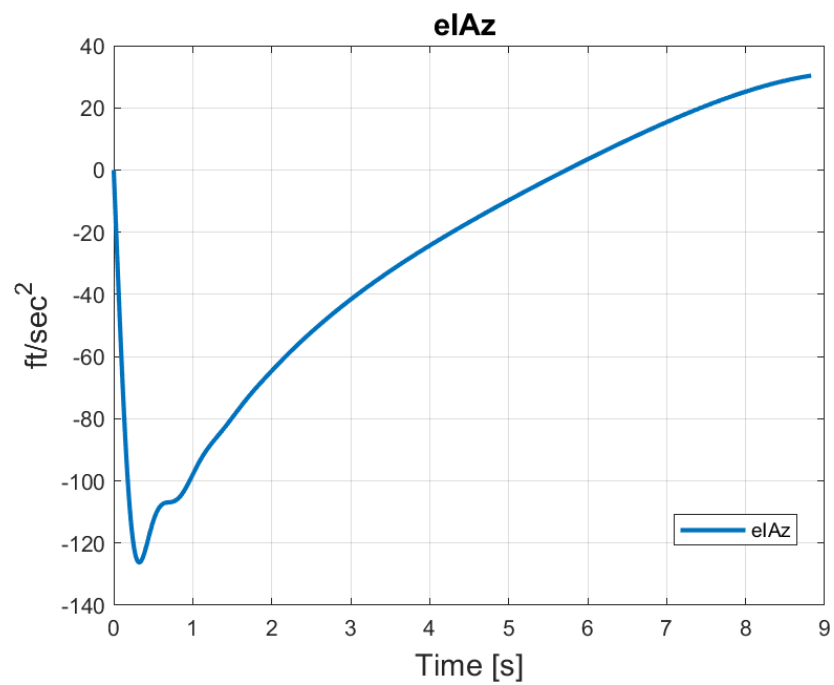


Figure 24  $e_{I,A_z}$  by pursuer.

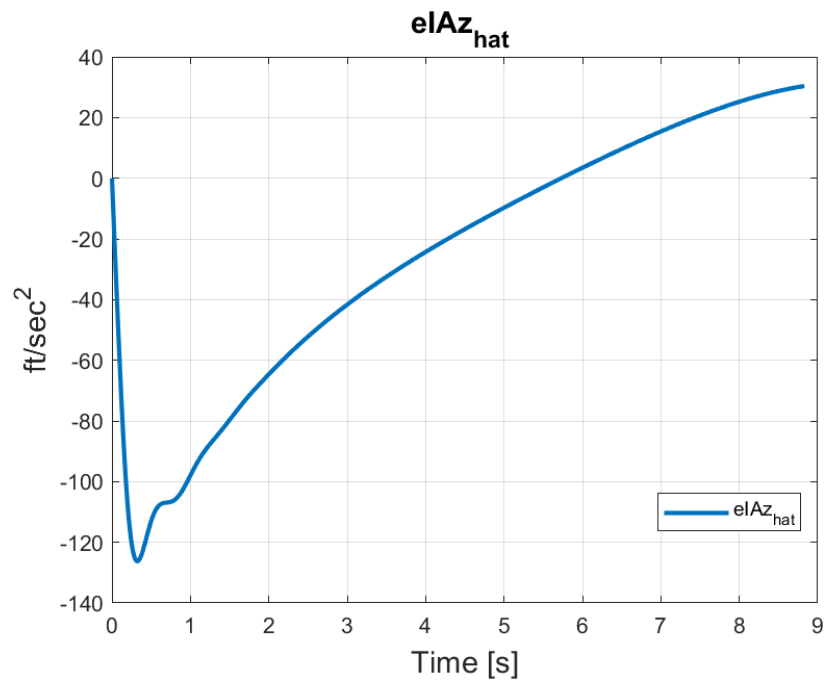


Figure 25  $\hat{e}_{I,A_z}$  by pursuer.

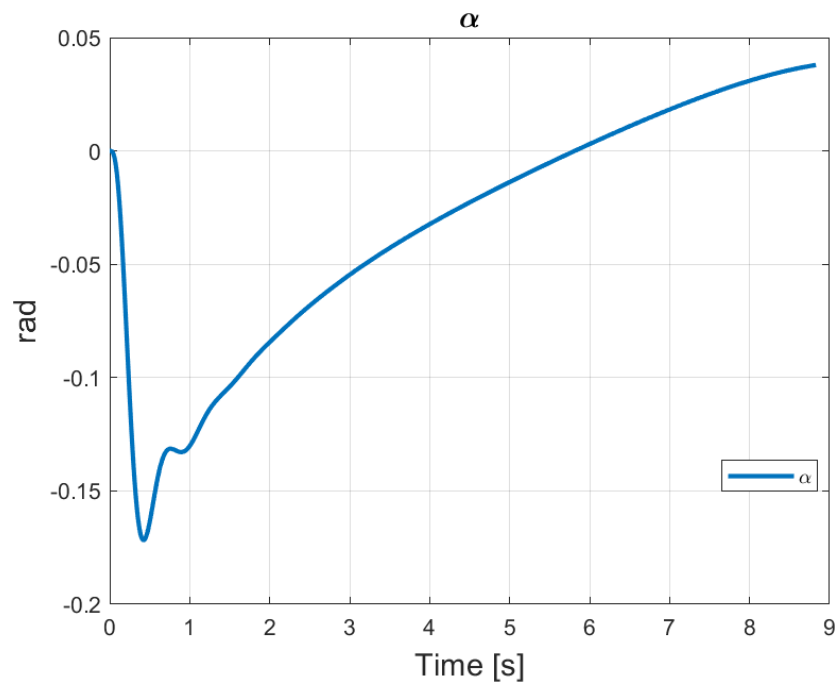


Figure 26  $\alpha$  by pursuer.

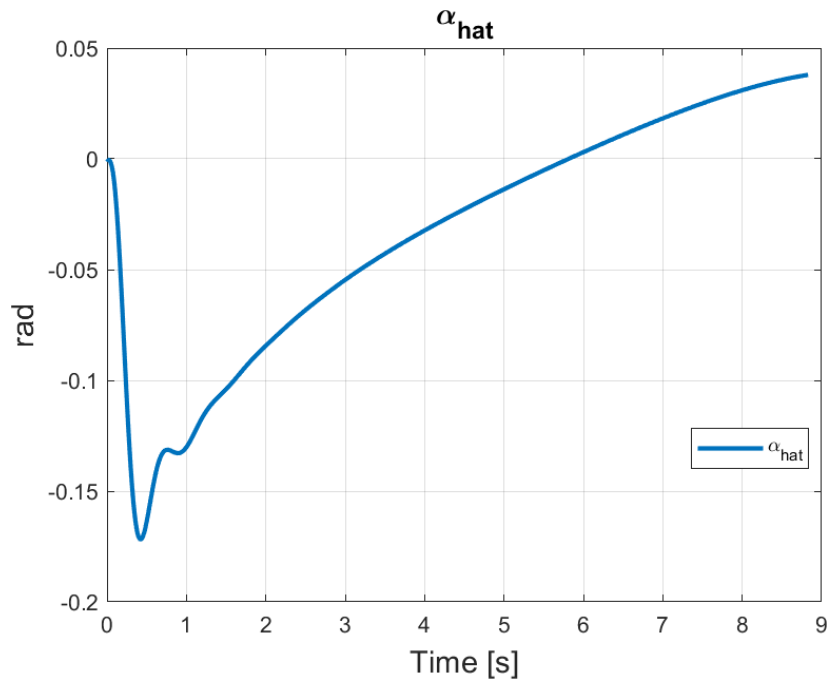


Figure 27  $\hat{\alpha}$  by pursuer.

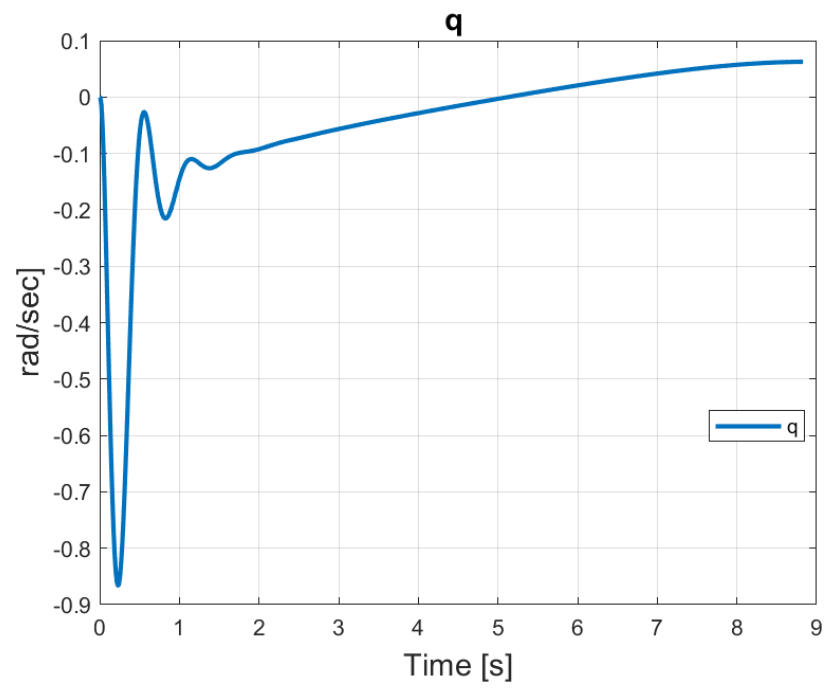


Figure 28  $q$  by pursuer.

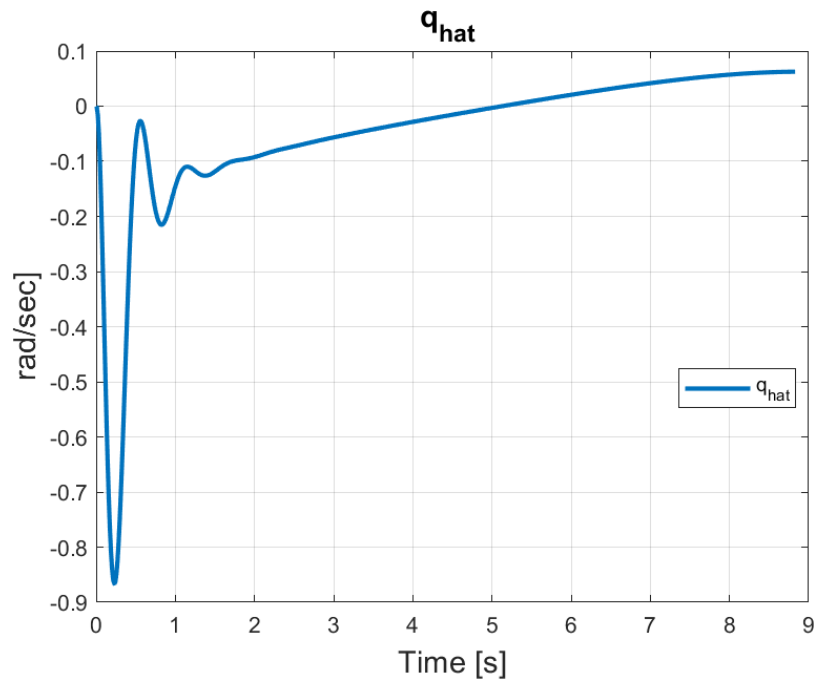


Figure 29  $\hat{q}$  by pursuer.

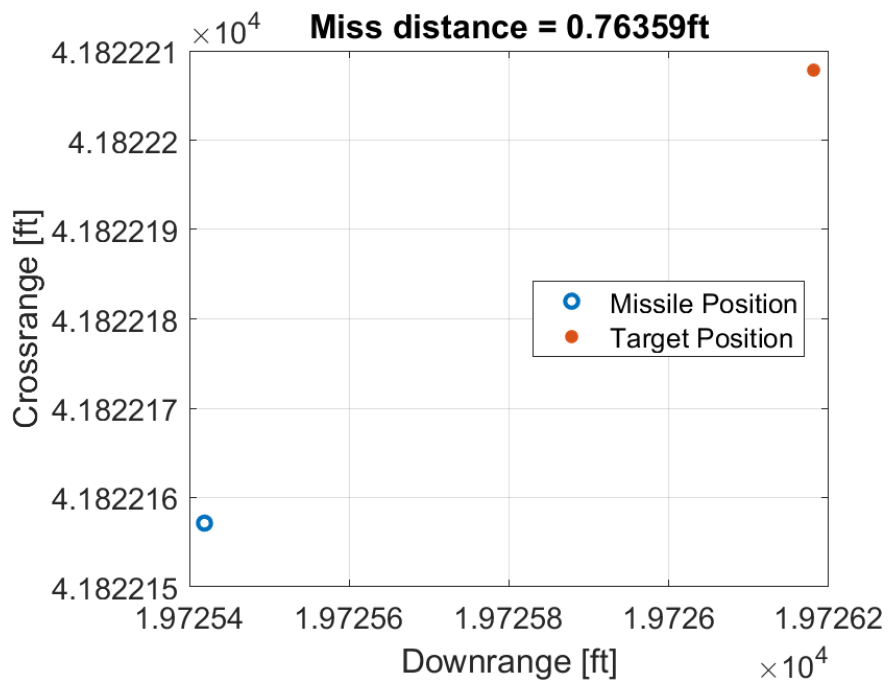


Figure 30 Missile and drone distance plot

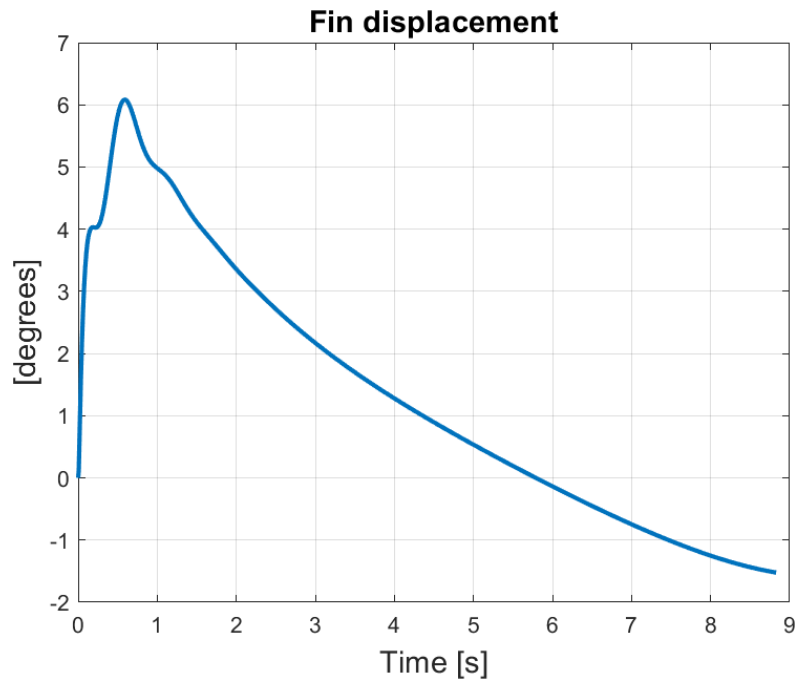


Figure 31 Fin displacement plot for Navigation guidance of Pursuer within the desired value of 35 degree.

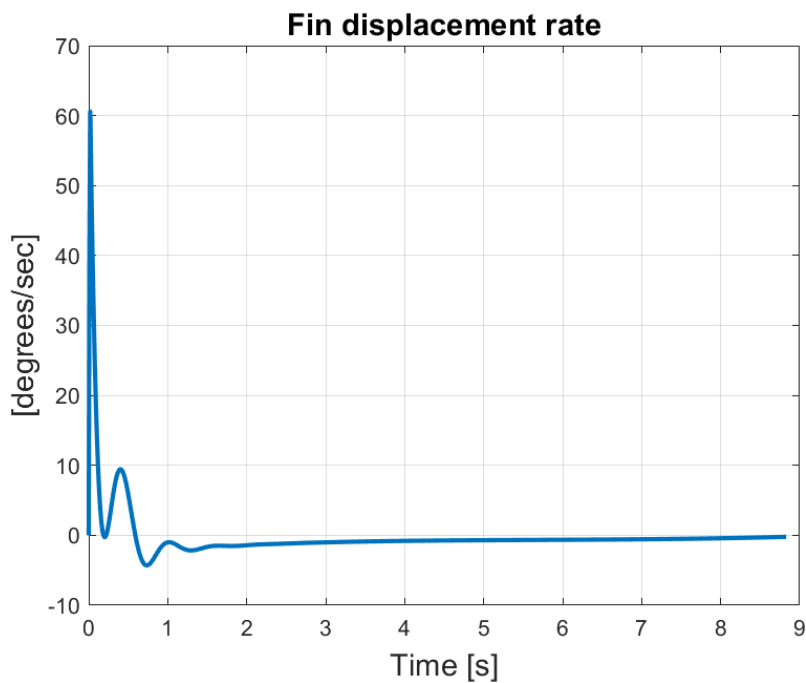


Figure 32 Fin displacement rate plot for Navigation guidance of Pursuer within the desired value of under 350 degree/sec.

**Conclusion:**

The MRAAM navigation and guidance system is designed, and all the parameters are proved to within the desired range. The LQR gain chosen was the 23rd penalty  $q_{eI} = 14.6158$  rad/sec and the  $q_0 = 19th\ iteration\ of\ 14.0170$  leading to the best achieved miss distance of 0.76359 ft. there furthermore scope to tune the observer and the controller by increasing the no. of penalty points in the same range. As well as the autopilot can be tuned to miss distance reduction as low as 0.001ft by proper iterative penalty selections and by considering the singularities in solver part.